Dynamic mechanical analysis on fused polymer optical fibers: towards sensor applications

Arnaldo Leal-Junior,[1,*] Anselmo Frizera,[1] Maria José Pontes,[1] Paulo Antunes,[2]
Nélia Alberto,[3] Maria Fátima Domingues,[2] Heeyoung Lee,[4] Ryo Ishikawa,[4] Yosuke Mizuno,[4]
Kentaro Nakamura,[4] Paulo André,[5] and Carlos Marques[2]

[1]Telecommunications Laboratory (LABTEL), Graduate Program of Electrical Engineering of Federal University of Espírito Santo, Vitória,
Espírito Santo, Brazil
[2]Instituto de Telecomunicações and Physics Department & I3N, University of Aveiro, Aveiro, Portugal
[3]Instituto de Telecomunicações and Centre for Mechanical Technology and Automation, Department of Mechanical Engineering,
Aveiro University, Aveiro, Portugal
[4]Institute of Innovative Research, Tokyo Institute of Technology, Tokyo, Japan
[5]Instituto de Telecomunicações and Department of Electrical and Computer Engineering, Instituto Superior Técnico,
University of Lisbon, Lisbon, Portugal
*Corresponding author: arnaldo.leal@aluno.ufes.br

This Letter presents, for the first time, to the best of our knowledge, the dynamic mechanical analysis of a polymer optical fiber (POF) that was previously damaged by the catastrophic fuse effect. The variation of the fiber Young's modulus was evaluated with respect to the increase of temperature, humidity, and frequency of strain cycles. The obtained data for the fused POF are compared with the ones for the same POF without the fuse effect. The results show the feasibility of the fused POF for sensor applications, such as strain and acceleration measurement, since it presents temperature sensitivity almost two times lower in temperatures between 26°C and 90°C and Young's modulus 2.3 times lower than those obtained with the bare fiber. The Young's modulus variation with the humidity is 1.5 MPa/%RH in a humidity range of 66–96%. In addition, the fused POF presented a variation of its dynamic modulus with the frequency increase four times lower than non-fused POFs on the range of 0.01–100.00 Hz. These results pave the way for future applications of fused POFs as sensing elements.   © 2018 Optical Society of America

The catastrophic fuse effect is the continuous self-destruction process of an optical fiber, triggered when high-power light is used in optical fibers under a tight bend or in damaged connections [1–4]. When the high-power optical signals propagating through the fiber find such defected points, this generally results in a local heating and the creation of an optical discharge. Such a discharge is captured in the fiber core and back-propagates towards the light source, permanently damaging the optical fiber. The first catastrophic fuse effect was reported in silica single-mode fibers (SMFs) in 1987 [4]. Since then, this effect has been reported in various special glass fibers, such as microstructured [5], fluoride [6], chalcogenide [6], erbium-doped [7], and photonic crystal [8] fibers. The fuse effect was first observed in polymer optical fibers (POFs) in 2014 [8], and its propagation mechanism was discussed in detail [8–10]. The reported threshold power density was 180 times lower than that of silica fibers, and the propagation velocity was about 0.02 m/s for the fuse effect on POFs, whereas this value can be about 0.5 m/s for silica fibers [11]. Furthermore, in POFs, the passing of the optical discharge leads to a dark oscillatory path with an almost constant period [10].

Since the optical propagation loss in fused silica fibers is extremely high, the fuse effect is a critical factor that limits the maximum optical power allowed in an optical fiber system for communication purposes [10]. In addition, this phenomenon restricts the application to distributed sensing, based on fiber nonlinear effects, such as Brillouin or Raman scattering [12,13]. However, the fuse effect in silica fibers also creates voids in the fiber, which are micro-cavities that can be employed as a cost-effective alternative for Fabry–Perot interferometer (FPI) applications, since these micro-cavities are usually manufactured with high cost equipment, such as femtosecond lasers [11]. For this reason, silica fibers with the catastrophic fuse effect have been used to produce sensors for measuring several parameters including strain [11], refractive index [14], relative humidity (RH) [15], temperature [16], and hydrostatic pressure [17]. Additionally, the produced micro-cavities can be employed as edge filters for low-cost interrogation of fiber Bragg grating sensors [18].

Although the reported applications were developed in silica fiber, POFs present advantages over silica fibers due to their

material features, which include higher fracture toughness, strain limits, and flexibility in bending [19]. Furthermore, the non-brittle nature and biocompatibility of POFs make them suitable for *in vivo* applications [20,21].

In order to discuss the fuse effect on POF material features for the first time, to the best of our knowledge, this Letter presents the dynamic mechanical analysis (DMA) on a POF before and after the catastrophic fuse effect. A stress-strain test is performed on the non-fused and fused POFs to measure their Young's modulus. Then temperature tests are made to evaluate the fiber viscoelastic properties, including the storage modulus means of increasing the temperature during sequential strain cycles. Furthermore, the fiber material behavior with frequency and temperature is also measured. Since the material characterization of the fused POFs is an important analysis that should be performed prior to their use as physical sensors, the results presented in this Letter can pave the way for future sensor applications of fused POFs, exploiting the polymer viscoelastic nature [22].

The fiber employed in the experiment is a perfluorinated graded index POF [23] with a core diameter of 50 μm, a cladding with 50 μm thickness, and an overcladding that results in a fiber total diameter of 750 μm (ID050 Seikisui Chemical, Japan). The materials of core and cladding are doped and undoped polyperfluorobutenylvinyl, either with a refractive index of 1.356 or 1.342, respectively. The setup employed for the fiber fuse initiation is presented in [8]. A distributed-feedback laser diode (output power of 5 mW; wavelength of 1546 nm) is amplified using an erbium-doped fiber amplifier (LXM-S-21, Luxpert Technologies) to 200 mW and injected into the POF. One end of the POF is connected to a silica SMF using an FC/SC adaptor. The other end is polished with a 0.5 μm alumina powder to obtain a high surface roughness for the fuse effect ignition. Since POF cleaving is important for the fiber connectorization [24], all samples were cleaved with a razor blade perpendicular to the fibers with controlled temperature of 70°C.

Polymers are viscoelastic materials that present a combination of loss and storage behavior on their responses [25], where such a behavior leads to a non-constant response with stress and strain cycles [26] that are also observed in a long-term cyclic response [27]. Moreover, their strain performance can be enhanced through annealing and etching treatments [28]. The annealing can be made in the fiber or in the preform [29] and is composed of keeping the fiber in a temperature below the fiber material glass transition temperature (T_g) for some hours [30,31]. In order to increase the strain performance of the POFs, the annealing is made on both non-fused and fused POFs, which were kept in a temperature of 90°C for 24 h. The annealing temperature was chosen considering that the employed POFs present a structure similar to CYTOP fibers, which presents a T_g of about 120°C. To characterize the response of the fibers under different conditions, DMA is performed, which is composed of the application of an oscillatory load on the polymer with specific temperature, frequency, and humidity range [32]. Thus, the non-fused and fused fibers are positioned on a dynamic mechanic analyzer (DMA 8000, Perkin Elmer, USA) for axial stress-strain cycles (see Fig. 1). The climatic chamber is composed of the DMA 8000 heater and cooling units for temperature control, and the TT humidity generator and controller (Triton Technology, USA), which
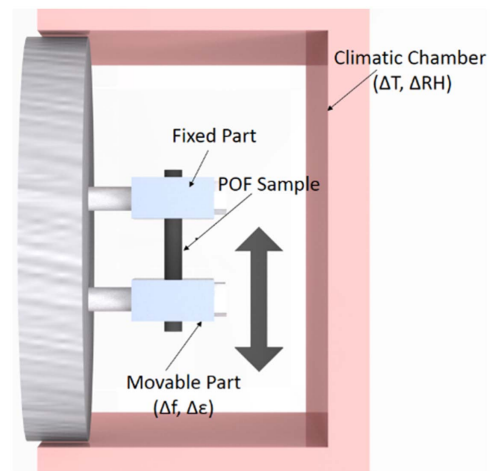

Fig. 1. Experimental setup employed for the DMA on the POFs.

enable the variation of the temperature (ΔT) and RH variation (ΔRH), while the movable part provides the frequency (Δf) and strain ($\Delta \varepsilon$) variations.

The analyzed material properties with the DMA are the storage moduli (E') and loss moduli (E''). The relation between these two moduli with the dynamic Young's modulus of a viscoelastic material (E^*) is presented as

$$E^* = E' + iE''. \tag{1}$$

The storage modulus is related to the elastic part of the response, and the loss modulus presents the dissipative or viscous part of the response.

The non-fused and fused fibers are also subjected to stress-strain tests to measure the material Young's moduli before and after the fuse effect. Then thermal tests in the range of 26–90°C are carried out to verify the material behavior with the temperature increase. In addition, frequency tests from 0.01 to 100.00 Hz are performed on the POFs under strain cycles to evaluate their response over the frequency increase. Finally, a ΔRH of about 30% (in the range from 66% to 96% due to operational limitations of the employed RH controller, since the RH variation range that provides the highest stability is about 30% for humidity sweep) is applied on the fibers to assess the material sensitivity with respect to this parameter. The storage modulus variation with the RH was also evaluated under three different temperatures (25°C, 55°C, and 75°C).

The stress-strain cycles made on the polymer enable the evaluation of the Young's modulus. The obtained Young's modulus of the non-fused fiber was 3.5 GPa, while the fiber after the fuse effect presents a Young's modulus of 1.5 GPa. These values were obtained by the slope of the stress-strain curve on the strain range of 0.05–0.25%, as recommended by ISO527-1:1996 for polymers. This reduction may be related to an additional relaxation of the polymer chains after the passage of the high-energy optical discharge that presents a temperature of about 3327°C [10]. The lower Young's modulus of the fused POF can provide higher sensitivity for strain sensing applications, when compared with the non-fused POF [33].

Figure 2 presents the response of the polymer material with the temperature increase. The temperature sensitivity obtained for the fused POFs is 6.25 MPa/°C, which is almost two times
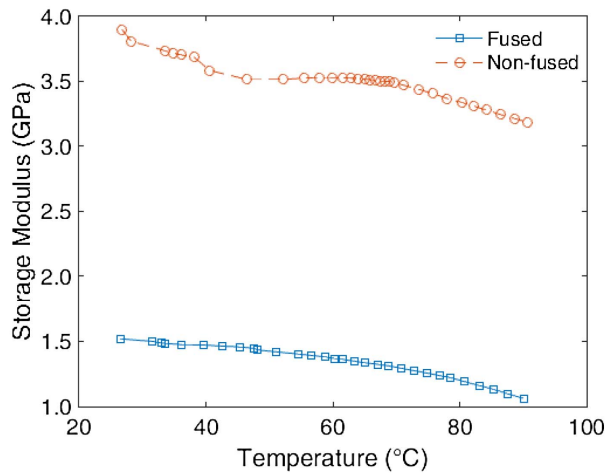
Fig. 2. Temperature response of fused and non-fused POFs.

Fig. 3. Frequency response of fused and non-fused POFs.

lower than the one of the non-fused POF (11.30 MPa/°C). These results were obtained with an RH of 88% (room RH due to operational limitations of the RH controller) in a frequency of 1 Hz and show that the fused POF presents a lower variation of the storage modulus with the increase of temperature, which provides advantages over the non-fused POF for intensity-variation-based sensor applications. This sensor interrogation technique relies on the optical power variation with respect to some parameters, such as strain [34], angle [22], and refractive index [35]. Therefore, a higher variation of the Young's modulus, caused by the change in the storage modulus, leads to a higher cross-sensitivity of the sensor with the temperature, which can be a source of errors on the sensor's measurement. Since the fused POF can propagate light for a few centimeters with an optical propagation loss of about 1.4 dB/cm [8], an intensity-variation-based sensor using the fused POF provides lower temperature cross-sensitivity than the one with the non-fused fiber. Such a high optical propagation loss is due to the fuse effect, since the loss of the non-fused POF is about 250 dB/km [10].

Regarding the frequency response of each fiber, Fig. 3 presents the results obtained for a load with a frequency range between 0.01 and 100.00 Hz with a step of three points per decade applied on POFs under constant temperature (26.0°C) and RH (88%), which corresponds to the room temperature and RH, respectively. The humidity controller was set to maintain the room RH due to operational limitations of its humidity range. The response of the non-fused fiber presents a considerable variation with the increase of frequency, which starts around 3.2 GPa when the frequency is 0.01 Hz and increases to 3.5 GPa when the frequency is 1 Hz. Then it presents an almost linear increase of 43.00 MPa/Hz for a frequency range from 1.00 to 100.00 Hz. The fused POF response presents a positive frequency dependence with a coefficient of 9.00 MPa/Hz (calculated in the range of 10 to 100 Hz), which is more than four times lower than that of the non-fused POF. Such advantageous findings also enable the use of fused POFs in sensors for low frequency applications.

This stable response of the fused POF with the increase of frequency is an advantage over the non-fused ones for applications, such as accelerometers operating at frequencies below
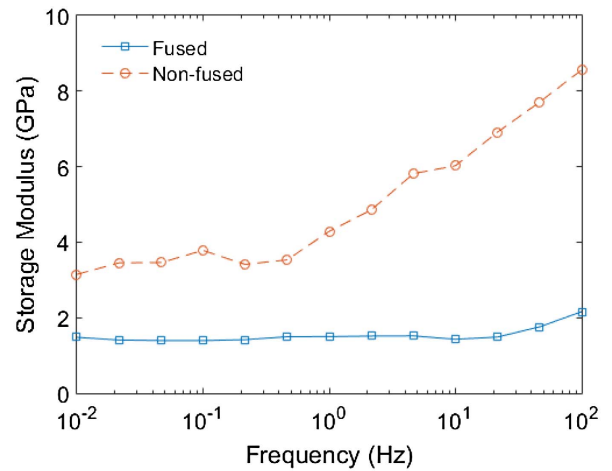
100.00 Hz [36]. In addition, it is useful for curvature sensor applications in different angular velocities [22], where such a lower variation on the mechanical properties of the fiber under strain will provide lower errors for the tests with a wider range of angular velocities.

The last set of tests made is the RH variation to verify the water absorption of the samples. Since the employed POF presents a material composition similar to cyclic transparent amorphous fluoropolymer (CYTOP) fibers [37], it is expected that such fibers do not change their mechanical properties with the increase of this parameter [37]. Such a humidity insensitivity can reduce the cross-sensitivity of POF sensors, which is often observed in polymethyl methacrylate (PMMA) POFs [31]. Figure 4 presents the storage modulus variation for the non-fused and fused POFs in an RH variation of about 30%. Such a variation was obtained due to operational limitations that lead to lower humidity variation in the climatic chamber. After setting the humidity, it remains constant for about 30 min before the test. Then the highest humidity is set on the equipment. In addition, the tests were made with
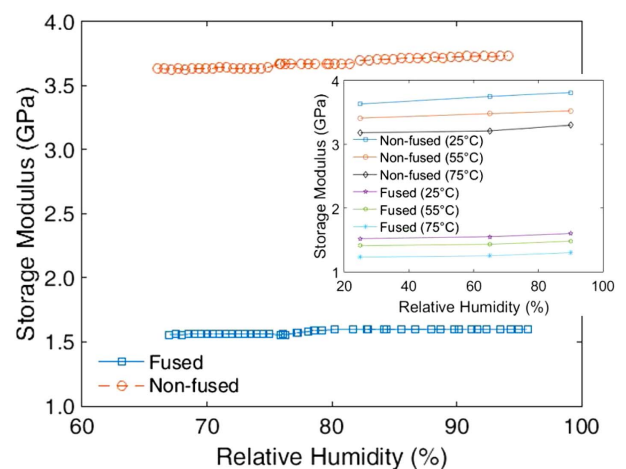

Fig. 4. Storage modulus as a function of RH of about 30% (from 66% to 96%) for the fused and non-fused POFs. The inset shows the storage modulus as a function of the RH at three different temperatures.

constant temperature of 26.0°C and frequency of 1 Hz, which is the standard frequency of the equipment for this type of test. In order to evaluate the POF response under low humidity conditions and for different temperatures, the inset in Fig. 4 presents the non-fused and fused POFs responses with three different temperatures, namely 25°C, 55°C, and 75°C, for three RH conditions (25%, 65%, and 90%).

Regarding water/moisture absorption, both non-fused and fused POFs presented low variations of their mechanical properties with the increase of humidity, as depicted in Fig. 4. The maximum variation for fused fibers was below 4.5 MPa, which means that the ΔRH may not lead to deviations on the measurement of fused POF sensor applications. Note that the variation of the storage modulus with the RH for the fused POF was similar to that for the non-fused POFs that enable sensing applications of both fused and non-fused POFs with lower humidity cross-sensitivity than the one of the PMMA POFs, for example. Furthermore, the obtained results under different temperatures and with lower RH also show the low absorption of the fused POFs, where the curves presented almost constant slope, and their offsets are due to the temperature variations. The advantages related to the material features of the fused POFs pave the way for sensor applications where the sensing element is the fused POF itself. This can be achieved since the POFs can propagate light for a few centimeters after the fuse effect.

In conclusion, this Letter presents the DMA of a fused POF. The material responses with respect to temperature, load frequency, and humidity were evaluated in detail. In addition, stress-strain tests were performed to obtain the Young's modulus of the fused POF, which is 2.3 times lower than the one of the bare POF. The results were compared with those obtained for a non-fused POF. The storage modulus of the fused POF presented a lower sensitivity two times lower than temperature variation, which may lead to lower temperature cross-sensitivity. Additionally, the fused POF presented a stable dynamic modulus with the frequency range of 0.01–100.00 Hz, with four times lower modulus variation than that of the non-fused POF. Furthermore, low variation with the increase of humidity was obtained for the fused POFs, where such a variation is lower than 1.5 MPa/%RH.

REFERENCES

1. R. Kashyap and K. J. Blow, Electron. Lett. **24**, 47 (1988).
2. R. M. Atkins, P. G. Simpkins, and D. Yablon, Opt. Lett. **28**, 974 (2003).
3. Y. Shuto, S. Yanagi, S. Asakawa, M. Kobayashi, and R. Nagase, IEEE J. Quantum Electron. **40**, 1113 (2004).
4. R. Kashyap, Opt. Express **21**, 6422 (2013).
5. E. M. Dianov, I. A. Bufetov, A. A. Frolov, Y. K. Chamorovsky, G. A. Ivanov, and I. L. Vorobjev, IEEE Photonics Technol. Lett. **16**, 180 (2004).
6. E. M. Dianov, I. A. Bufetov, A. A. Frolov, V. M. Mashinsky, V. G. Plotnichenko, M. F. Churbanov, and G. E. Snopatin, Electron. Lett. **38**, 783 (2002).
7. F. Domingues, A. R. Frias, P. Antunes, A. O. P. Sousa, R. A. S. Ferreira, and P. S. André, Electron. Lett. **48**, 1295 (2012).
8. Y. Mizuno, N. Hayashi, H. Tanaka, K. Nakamura, and S. Todoroki, Appl. Phys. Lett. **104**, 043302 (2014).
9. Y. Mizuno, N. Hayashi, H. Tanaka, and K. Nakamura, IEEE Photonics J. **6**, 6600307 (2014).
10. Y. Mizuno, N. Hayashi, H. Tanaka, K. Nakamura, and S. Todoroki, Sci. Rep. **4**, 4800 (2014).
11. P. F. C. Antunes, M. F. F. Domingues, N. J. Alberto, and P. S. André, IEEE Photonics Technol. Lett. **26**, 78 (2014).
12. Y. Mizuno and K. Nakamura, Appl. Phys. Lett. **97**, 021103 (2010).
13. Y. Mizuno, N. Hayashi, H. Fukuda, K. Y. Song, and K. Nakamura, Light Sci. Appl. **5**, e16184 (2016).
14. M. F. Domingues, P. Antunes, N. Alberto, R. Frias, R. A. S. Ferreira, and P. André, Measurement **77**, 265 (2016).
15. N. Alberto, C. Tavares, M. F. Domingues, S. F. H. Correia, C. Marques, P. Antunes, J. L. Pinto, R. A. S. Ferreira, and P. S. André, Opt. Quantum Electron. **48**, 1 (2016).
16. M. F. Domingues, P. Antunes, N. Alberto, A. R. Frias, A. R. Bastos, R. A. S. Ferreira, and P. S. André, Microw. Opt. Technol. Lett. **57**, 972 (2015).
17. M. F. Domingues, T. De Brito Paixão, E. F. T. Mesquita, N. Alberto, A. R. Frias, R. A. S. Ferreira, H. Varum, P. F. Da Costa Antunes, and P. S. De Brito André, IEEE Sens. J. **15**, 5654 (2015).
18. C. Díaz, C. Leitão, C. Marques, M. Domingues, N. Alberto, M. Pontes, A. Frizera, M. Ribeiro, P. André, and P. Antunes, Sensors **17**, 2414 (2017).
19. K. Peters, Smart Mater. Struct. **20**, 13002 (2011).
20. W. Yuan, L. Khan, D. J. Webb, K. Kalli, H. K. Rasmussen, A. Stefani, and O. Bang, Opt. Express **19**, 19731 (2011).
21. H. U. Hassan, J. Janting, S. Aasmul, and O. Bang, IEEE Sens. J. **16**, 8483 (2016).
22. A. G. Leal-Junior, A. Frizera, and M. J. Pontes, J. Lightwave Technol. **36**, 1112 (2018).
23. Y. Koike and M. Asai, NPG Asia Mater. **1**, 22 (2009).
24. A. Stefani, K. Nielsen, H. K. Rasmussen, and O. Bang, Opt. Commun. **285**, 1825 (2012).
25. A. G. Leal Junior, A. Frizera, and M. J. Pontes, Opt. Laser Technol. **93**, 92 (2017).
26. A. Stefani, S. Andresen, W. Yuan, N. Herholdt-Rasmussen, and O. Bang, IEEE Photonics Technol. Lett. **24**, 763 (2012).
27. I.-L. Bundalo, K. Nielsen, G. Woyessa, and O. Bang, Opt. Mater. Express **7**, 967 (2017).
28. A. Pospori, C. A. F. Marques, D. Sáez-Rodríguez, K. Nielsen, O. Bang, and D. J. Webb, Opt. Fiber Technol. **36**, 68 (2017).
29. C. A. F. Marques, A. Pospori, G. Demirci, O. Çetinkaya, B. Gawdzik, P. Antunes, O. Bang, P. Mergo, P. André, and D. J. Webb, Sensors **17**, 891 (2017).
30. W. Yuan, A. Stefani, M. Bache, T. Jacobsen, B. Rose, N. Herholdt-Rasmussen, F. K. Nielsen, S. Andresen, O. B. Sørensen, K. S. Hansen, and O. Bang, Opt. Commun. **284**, 176 (2011).
31. G. Woyessa, K. Nielsen, A. Stefani, C. Markos, and O. Bang, Opt. Express **24**, 1206 (2016).
32. A. Badawi, J. Mater. Sci. Mater. Electron. **26**, 3450 (2015).
33. X. Hu, C.-F. J. Pun, H.-Y. Tam, P. Mégret, and C. Caucheteur, Opt. Express **22**, 18807 (2014).
34. K. S. C. Kuang, W. J. Cantwell, and P. J. Scully, Meas. Sci. Technol. **13**, 1523 (2002).
35. A. R. Prado, A. G. Leal-Junior, C. Marques, S. Leite, G. L. de Sena, L. C. Machado, A. Frizera, M. R. N. Ribeiro, and M. J. Pontes, Opt. Express **25**, 30051 (2017).
36. A. Stefani, S. Andresen, W. Yuan, and O. Bang, IEEE Sens. J. **12**, 3047 (2012).
37. A. Lacraz, M. Polis, A. Theodosiou, C. Koutsides, and K. Kalli, IEEE Photonics Technol. Lett. **27**, 693 (2015).